SIAM REVIEW
Vol. 24, No. 2, April 1982

© 1982 Society for Industrial and Applied Mathematics
0036/1445/82/2402-0001 $01.00/0

GROUP VELOCITY IN FINITE DIFFERENCE SCHEMES*

LLOYD N. TREFETHEN†

Abstract. The relevance of group velocity to the behavior of finite difference models of time-dependent partial differential equations is surveyed and illustrated. Applications involve the propagation of wave packets in one and two dimensions, numerical dispersion, the behavior of parasitic waves, and the stability analysis of initial boundary value problems.

CONTENTS

Introduction. It has long been recognized by physicists and engineers that energy propagation under dispersive partial differential equations is governed by the quantity known as group velocity [1], [3], [4], [11], [12], [19]. By a dispersive equation we mean one that admits plane wave solutions of the form $\exp[i(\omega t - \xi x)]$, but with the property that the speed of propagation of these waves is not independent of ξ. Now, even if an equation is nondispersive, any discrete model of it will be dispersive. For this reason group velocity is essential to understanding the behavior of numerical models of partial differential equations, a fact which has been insufficiently recognized by numerical analysts. The purpose of this paper is to substantiate this claim by presenting a variety of applications of group velocity in the study of finite difference schemes. We will not consider finite elements and related methods, but the same principles apply.

Previous discussions of group velocity for finite difference methods are surprisingly few and scattered. The papers of Vichnevetsky [16], [17], however, contain many of the ideas that will occupy our first three sections. Group velocity also figures in the work of Chin and Hedstrom, notably in [7], and the paper by Bamberger et al. [2] studies group velocity errors in two dimensions. Probably none of the material here is new, with the possible exception of some observations about stability in § 5, but it is difficult to trace antecedents.

There is one major limitation to the group velocity analysis: it applies directly only to nondissipative difference schemes. Any dissipation introduces a frequency-dependent attenuation of Fourier components that makes the analysis of wave propagation more complicated [4]. Nevertheless, under many common difference methods (e.g., Lax-Wendroff) dispersion dominates dissipation at low frequencies, and then the predictions of group velocity for low-frequency components are approximately valid.

This paper is divided into six sections. Section 1 derives the general formula for group velocity and also derives the dispersion relations for three simple difference

* Received by the editors April 2, 1981, and in final revised form July 9, 1981. This work was supported in part by a Hertz Foundation Fellowship and in part by the Office of Naval Research under contract N00014-75-C-1132.

† Computer Science Department, Stanford University, Stanford, California 94305.

schemes. Section 2 considers group velocity in the context most familiar to a physicist—the propagation in one dimension of pulses, wave packets and wave fronts. This amounts to a study of the deviation from linearity of numerical dispersion relations near the (ξ, ω) origin. Section 3 considers the generation and propagation of parasitic waves by difference schemes, and the reflection and transmission of waves at interfaces. These matters involve the outlying regions of the dispersion relation near $\xi = \pm\pi/h$ and/or $\omega = \pm\pi/k$. (h and k are the spatial and temporal step sizes, respectively.) Section 4 discusses group velocity in two dimensions—where the finite difference model introduces not only dispersion, but anisotropy. Section 5 shows that there is a natural connection between the stability of difference methods for initial boundary value problems and the group velocity of parasitic waves. Finally, § 6 gives a brief discussion and a summary of the earlier sections.

1. Dispersion relations and group velocity. Let us begin by sketching the derivation of the group velocity in one space dimension by a stationary phase argument, which is due to Lord Kelvin. (This and other explanations of group velocity are excellently presented in the books of Brillouin [3], [4], Lighthill [12], and Whitham [19].) Suppose that a scalar, linear partial differential equation with constant coefficients admits solutions of the form

$$u(x, t) = e^{i(\omega t - \xi x)}. \tag{1.1}$$

For each real *wave number* ξ, assume there is a corresponding real *frequency* ω such that (1.1) is a solution. The relation

$$\omega = \omega(\xi) \tag{1.2}$$

is called the *dispersion relation* for the differential equation. Now it is obvious that (1.1) propagates rightward with t at the speed

$$c(\xi) = \frac{\omega(\xi)}{\xi}, \tag{1.3}$$

which is called the *phase speed.* But the evolution of a wave packet containing several wave numbers will be more complicated. Let an initial distribution $f(x, 0)$ located approximately at the origin have the Fourier transform $F(\xi)$. Then at time $t \geqq 0$, the solution (ignoring normalization factors) can be written

$$f(x, t) = \int_{-\infty}^{\infty} F(\xi)\, e^{i(\omega(\xi)t - \xi x)}\, d\xi = \int_{-\infty}^{\infty} F(\xi)\, e^{it(\omega(\xi) - \xi x/t)}\, d\xi. \tag{1.4}$$

Suppose x/t is held fixed as $t \to \infty$. This corresponds to moving our eyes rightward at a fixed speed $x/t = \text{const}$. After a long time, what will we see? The answer comes from observing that as t increases, the exponential in (1.4) oscillates more and more rapidly with ξ, hence tends to cancel to 0 as $t \to \infty$. Such cancellation will evidently take place everywhere except for any ξ of stationary phase, at which

$$\frac{d}{d\xi}\left(\omega(\xi) - \frac{\xi x}{t}\right) = 0,$$

i.e.,

$$\frac{d\omega}{d\xi} = \frac{x}{t}.$$

As $t \to \infty$, therefore, our eyes will see only any wave numbers that satisfy this equation.

In other words, energy associated with wave number ξ moves asymptotically at the *group speed*

$$C(\xi) = \frac{d\omega}{d\xi}(\xi). \tag{1.5}$$

Consider now the simplest hyperbolic problem, the one-dimensional wave equation

$$u_t = -u_x. \tag{1.6}$$

This equation is nondispersive: its dispersion relation is the linear equation

$$\omega(\xi) = \xi, \tag{1.7}$$

and therefore $c(\xi) \equiv C(\xi) \equiv 1$. Let (1.6) be modeled by a linear finite difference scheme implemented on a uniform x-t grid with mesh size $h > 0$ in the x direction and $k > 0$ in the t direction, related by a mesh ratio $\lambda = k/h$. Let U_ν^n denote the numerical solution obtained at $(x, t) = (\nu h, nk)$. For each jh let $D_0(jh)$ denote the centered difference operator in x,

$$[D_0(jh)U^n]_\nu = \frac{1}{2jh}[U^n_{\nu+j} - U^n_{\nu-j}].$$

Familar difference schemes that we will consider are *leap frog*,

$$\text{LF:} \quad U^{n+1} - U^{n-1} = -2kD_0(h)U^n, \tag{1.8a}$$

Crank-Nicolson (an implicit scheme),

$$\text{CN:} \quad U^{n+1} - U^n = -\frac{k}{2}D_0(h)(U^n + U^{n+1}), \tag{1.8b}$$

and *fourth-order leap frog* (fourth order in space, second order in time),

$$\text{LF4:} \quad U^{n+1} - U^{n-1} = -2k[\tfrac{4}{3}D_0(h) - \tfrac{1}{3}D_0(2h)]U^n. \tag{1.8c}$$

Any of these difference schemes, like the original equation (1.6), imposes a relation between values of ξ and ω. To determine what the relation is, one need only insert the solution (1.1) in the difference formula and cancel common factors. The dispersion relations turn out to be

$$\text{LF:} \quad \sin \omega k = \lambda \sin \xi h, \tag{1.9a}$$

$$\text{CN:} \quad 2 \tan \frac{\omega k}{2} = \lambda \sin \xi h, \tag{1.9b}$$

$$\text{LF4:} \quad \sin \omega k = \frac{4\lambda}{3} \sin \xi h - \frac{\lambda}{6} \sin 2\xi h. \tag{1.9c}$$

The most fundamental difference between these relations and (1.7) is that because the grid is discrete, they are multiple-valued and 2π-periodic in ξh and ωk. It is enough to consider the fundamental domain $(\xi, \omega) \in [-\pi/h, \pi/h] \times [-\pi/k, \pi/k]$; any other frequency is an alias of a frequency in this domain. The second important feature of (1.9) is that each relation is dispersive. Near $(\xi, \omega) = (0, 0)$, $\omega(\xi) \approx \xi$, but away from this origin the dependence is far from linear. Figure 1 shows the dispersion relations for LF, CN, and LF4 plotted for mesh ratio $\lambda = 0.5$. By (1.5) the slope at any point (ξ, ω) is the group velocity for the corresponding wave (1.1). Because these curves

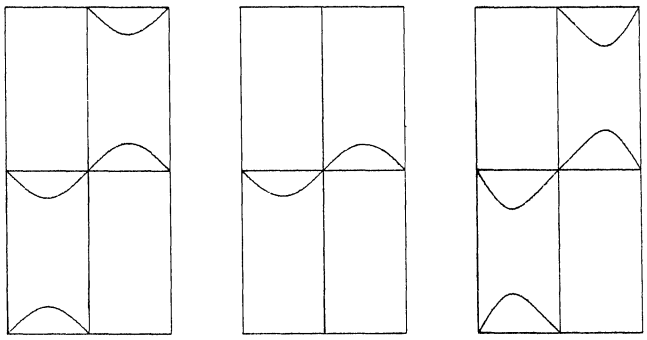

(a) LF (b) CN (c) LF4

FIG. 1. *Dispersion relations for difference models* LF, CN *and* LF4 *of* $u_t = -u_x$, *plotted for mesh ratio* $\lambda = .5$. *Each plot shows the region* $[-\pi/h, \pi/h] \times [-\pi/k, \pi/k]$ *of* (ξ, ω)*-space. The slope of the curve at a point* (ξ, ω) *is the group velocity for energy of that wave number and frequency. Consistency requires that each curve have slope* 1 *at the origin.*

are not straight lines through the origin, wave packets will disperse under any of these schemes, and understanding their behavior will require the consideration of group speed.

2. Pulses, wave packets and wave fronts. For a direct observation of group speed, it is simplest to look at a wave packet as in Fig. 2a. The region shown is the interval $[0, 3]$, on which a mesh of size $h = \frac{1}{160}$ has been placed. The initial packet is a sine wave modulated by a Gaussian centered at $x = \frac{1}{2}$,

$$u(x, 0) = e^{-16(x-1/2)^2} \sin \xi x,$$

with ξ chosen so that there are 8 grid points per wavelength: $\xi h = 2\pi/8 \approx .79$, $\xi \approx 125.7$. The exact solution of (1.6) should move right at speed 1. Figure 2b shows the actual result after the packet has propagated to $t = 2$ under LF with $\lambda = 0.4$. (The exact solution was used to provide values at $t = k$.) Instead of having reached $x = 2.5$, the packet is centered at $x \approx 1.97$, having traveled at speed roughly 0.74.

This is just the group speed for $\xi h = 2\pi/8$ under LF. First let us confirm that it

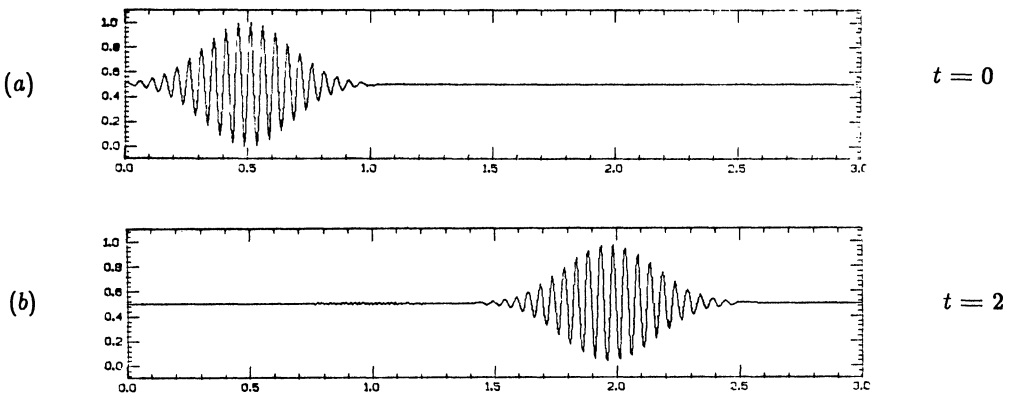

FIG. 2. *Propagation of a wave packet with* $\xi h \approx .79$ *under* $u_t = -u_x$ *modeled by* LF *with* $\lambda = .4$. *The packet moves not at the ideal speed* 1, *but at the group speed* $C \approx .74$.

is not the phase speed. Applying (1.3) to (1.9) gives

$$\text{(2.1a)} \qquad \text{LF:} \quad c(\xi) = \frac{1}{\lambda \xi h} \sin^{-1}(\lambda \sin \xi h) \approx 1 - \frac{1-\lambda^2}{6}(\xi h)^2,$$

$$\text{(2.1b)} \qquad \text{CN:} \quad c(\xi) = \frac{2}{\lambda \xi h} \tan^{-1}\left(\frac{\lambda}{2} \sin \xi h\right) \approx 1 - \frac{2+\lambda^2}{12}(\xi h)^2,$$

$$\text{(2.1c)} \qquad \text{LF4:} \quad c(\xi) = \frac{1}{\lambda \xi h} \sin^{-1}\left(\frac{4\lambda}{3} \sin \xi h - \frac{\lambda}{6} \sin 2\xi h\right) \approx 1 + \frac{\lambda^2}{6}(\xi h)^2.$$

(In each case "$\approx$" indicates equality up to $O((\xi h)^4$.) Equation (2.1a) predicts a phase speed $c \approx .91$ for the present problem, and clearly this does not account for Fig. 2b. On the other hand applying (1.5) to (1.9) gives the group speeds

$$\text{(2.2a)} \qquad \text{LF:} \quad C(\xi) = \frac{\cos \xi h}{\sqrt{1-\lambda^2 \sin^2 \xi h}} \approx 1 - \frac{1-\lambda^2}{2}(\xi h)^2,$$

$$\text{(2.2b)} \qquad \text{CN:} \quad C(\xi) = \frac{\cos \xi h}{1+\lambda^2 \sin^2 \xi h/4} \approx 1 - \frac{2+\lambda^2}{4}(\xi h)^2,$$

$$\text{(2.2c)} \qquad \text{LF4:} \quad C(\xi) = \frac{\frac{4}{3}\cos \xi h - \frac{1}{3}\cos 2\xi h}{\sqrt{1-(4\lambda \sin \xi h/3 - \lambda \sin 2\xi h/6)^2}} \approx 1 + \frac{\lambda^2}{2}(\xi h)^2.$$

To order $(\xi h)^2$ each C is 3 times as far from 1 as the corresponding c; this factor would become 5 for a scheme fourth-order accurate in both space and time, 7 for a sixth-order scheme, and so on. For the experiment of Fig. 2, (2.2a) predicts $C \approx .737$, just what was observed.

This simple example demonstrates the principle that makes analysis of group velocity errors in difference schemes worthwhile: there is more to the inaccuracy of a difference scheme than truncation error. The wave in Fig. 2b differs completely from the correct solution pointwise, and so an estimate of accumulated truncation error would lead to the conclusion that the computation had been useless. But in fact, it has been qualitatively correct. Errors caused by differencing are not random perturbations, but a systematic superposition of dispersions and possibly dissipations of various orders. Understanding behavioral features such as group velocity errors can yield various benefits: it can help one recognize that a mesh has been too coarse by the nature of the numerical solution produced; it can guide the initial choice of difference scheme and mesh size to minimize such errors; and it can enable one to make the most of an imperfect solution when further refinement of the mesh would be too expensive.

However, note that although the packet in Fig. 2 has moved 26% too slowly, it has broadened very little between $t = 0$ and $t = 2$—less than 10%. A packet disperses with time only to the extent that its Fourier transform is broad enough to include wave numbers whose group speeds differ significantly, and in this case the Fourier transform is a fairly narrow spike. Thus the absence of conspicuous dispersion in a wave packet is no guarantee that it has traveled at the right speed.

To focus on the dispersion of different wave numbers we can observe the propagation of a signal that is thoroughly polychromatic, such as the pulse of Fig. 3a (cf. [17]). This experiment takes place in the same laboratory as the last one: $x \in [0, 3]$, $h = \frac{1}{160}$, $\lambda = 0.4$, scheme = LF. But the initial distribution is now

$$u(x, 0) = e^{-3200(x-1/2)^2},$$

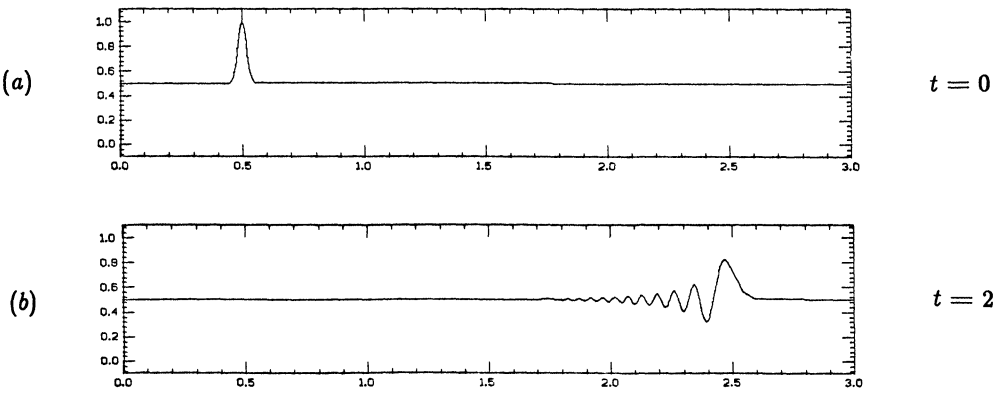

FIG. 3. *Propagation and dispersion of a narrow pulse under* $u_t = -u_x$ *modeled by* LF *with* $\lambda = .4$. *Higher wave numbers have lower group speeds and lag behind the main signal.*

which is much narrower than before and has central wave number $\xi = 0$. Since the pulse is narrow, its transform is broad, and Fig. 3b shows that it disperses quickly into a train of oscillations. Such oscillatory effects of finite difference schemes are common and well known. What is interesting from our point of view is to see how much of the oscillation can be predicted by considering group speed. At the front of the wave train, the low wave numbers travel at speed nearly 1, as they must. The further back one looks, the higher the wave number one sees; measurements in an enlargement of Fig. 3b confirm that the relationship is that of (2.2a). This example illustrates that group speed may help explain effects introduced by finite difference schemes even when the problem being modeled does not contain waves.

Group speed is only a first step in the analysis of a problem as in Fig. 3. More precise statements involving amplitudes as well as wave numbers can be arrived at by extending the stationary phase argument of § 1 to a steepest descent integration that takes into account the nature of $F(\xi)$ as well as the exponential in (1.4). In this manner Chin and Hedstrom have derived excellent estimates in terms of generalized Airy functions for the dispersion of point discontinuities as they propagate [6]. For many purposes, however, the much simpler consideration of group speeds will suffice.

The last two examples involve the propagation of a signal whose initial spatial distribution is given. Equally important are problems in which the temporal behavior of the signal at a boundary is primary. For example, Fig. 4 shows an experiment in which a sinusoidal forcing oscillation at the left boundary radiates a wave into the

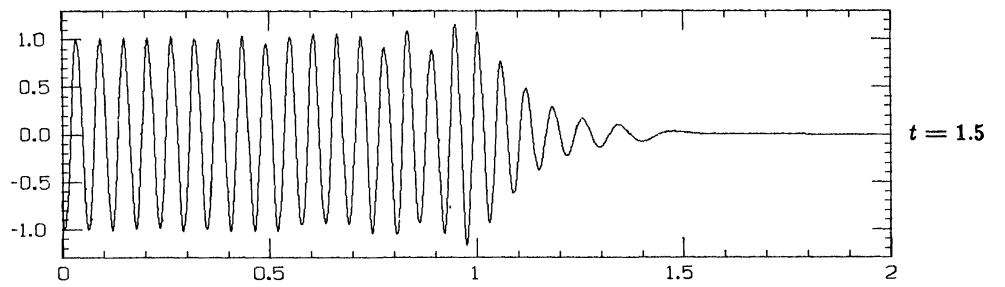

FIG. 4. *Propagation of a wave forced at the left boundary with* $\omega k = 1$ *under* $u_t = -u_x$ *modeled by* CN *with* $\lambda = 5$. *The wave front travels at the group speed* $C \approx .75$.

interior of the interval [0, 2] (cf. [16]). Here $h = 1/500$, $\lambda = 5$, and the scheme is CN. The wave

$$u(0, t) = \sin 100t$$

has been turned on at $t = 0$. At $t = 1.5$, only a low-frequency forerunner has reached $x = 1.5$; the main oscillation of amplitude 1 has reached only $x = 1.0$ or 1.1, suggesting that the wave front propagates at a speed roughly 0.7. Now to analyze a problem like this we need to know how C depends on ω, not ξ. Instead of (2.2b), therefore, we need the formula

$$\text{(2.3)} \qquad \text{CN:} \qquad C(\omega) = \cos^2 \frac{\omega k}{2} \sqrt{1 - \left(\frac{2}{\lambda}\right)^2 \tan^2 \frac{\omega k}{2}},$$

which can be derived by solving (1.9b) for $\xi(\omega)$ instead of $\omega(\xi)$ and then setting $C = [d\xi/d\omega]^{-1}$. For the given problem $\omega k = 1$, and (2.3) predicts $C \approx .75$. This explains Fig. 4.

These examples show that, depending on the application, either $C = C(\xi)$ or $C = C(\omega)$ may be required. Both (2.2b) and (2.3) are unattractively complicated, however, compared to the mixed forms

$$\text{(2.4a)} \qquad \text{LF:} \qquad C = \frac{\cos \xi h}{\cos \omega k},$$

$$\text{(2.4b)} \qquad \text{CN:} \qquad C = \cos \xi h \cos^2 \frac{\omega k}{2},$$

$$\text{(2.4c)} \qquad \text{LF4:} \qquad C = \frac{\frac{4}{3} \cos \xi h - \frac{1}{3} \cos 2\xi h}{\cos \omega k},$$

which follow directly from (1.9) if one differentiates implicitly on both sides, rather than solving first for ω or ξ. These mixed forms show the separate effects of time and space differencing as plainly as possible, and their simplicity often makes them the best equations to use in calculations involving group velocity, at least during the intermediate steps. Indeed, with more complicated difference formulas it would often be impossible to solve the dispersion relation for ω or ξ, except numerically.

3. Parasites, interfaces and mesh refinement. The last section showed that since the dispersion relation of a finite difference scheme is not exactly linear near the (ξ, ω)-origin, waves whose wavelength is not large compared to the mesh travel at false speeds and disperse. Now we move to questions related to parasitic waves, which are artificially generated rather than part of the given problem, and whose frequencies lie near the extremes $\xi = \pm\pi/h$ or $\omega = \pm\pi/k$. Parasitic waves are completely non-physical, but still propagate according to the group velocity. For related discussions see [3], [7], [17].

Figure 5 shows a typical appearance of a parasite. The domain is $[-1, 1]$ with $h = .01$, $\lambda = .5$. On $[-1, 0]$ the equation $u_t = -u_x$ is modeled by LF4. At $x = 0$ this changes abruptly to $u_t = -.7u_x$ on $(0, 1]$, modeled by LF4 with the obvious change of coefficient. (A more careful scheme would use modified difference formulas at the interface [14].) At $t = 0$ a forcing function

$$u(-1, t) = \sin 40t$$

is turned on at the left boundary, and this oscillation generates a wave slow enough to be well represented in the given mesh. At $t = 1$ the wave encounters the interface.

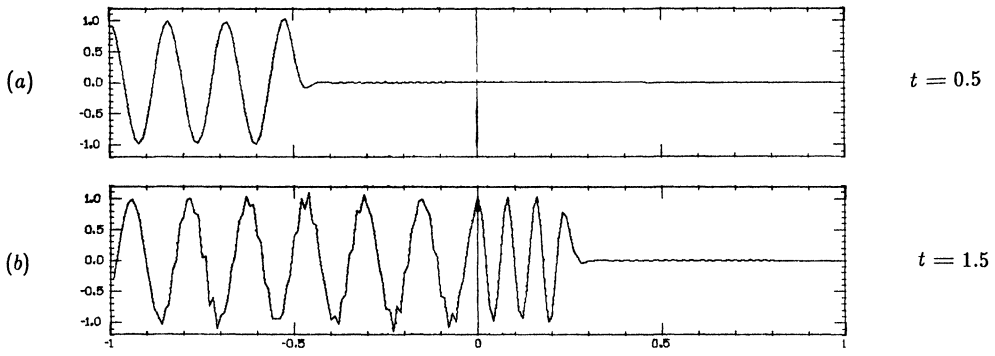

FIG. 5. *Generation of a leftgoing parasite at an interface between* $u_t = -u_x$ *and* $u_t = -.7u_x$, *both modeled by* LF4 *with* $\lambda = .5$. *The wave is forced with* $\omega k = 0.2$ *at the left boundary. The parasite travels left at speed* $C \approx -.80$.

The exact solution would continue through with no change but an increase in wave number, but the finite difference scheme introduces a reflected parasite of high wave number, which appears as wiggles in $[-.8, 0]$ in Fig. 5b. Similar (though polychromatic) parasites often appear in problems where the solution has traveling shocks or other discontinuities [7], [17].

The fundamental principle to use in analyzing this problem is that in the steady solution obtained after the initial transients have died down, ω must be the same everywhere. What sine waves of frequency ω can LF4 support? Figure 1c gives the answer: a small positive ω can correspond to two values of ξ, one near 0 and one near π/h. The former has $C \approx 1$. The latter must have $C \approx -\frac{5}{3}$, for the slope of the dispersion relation is $-\frac{5}{3}$ at $\xi = \pi/h$ (cf. (2.2c)). Returning to Fig. 5b, one sees that the reflected parasite has indeed traveled at speed roughly $-\frac{5}{3}$ from $t = 1$ to $t = 1.5$. Incidentally, it would be an easy matter to predict the amplitude of the parasite, but this is only indirectly related to group velocity.

In a problem like this the notion of phase speed would be not just inadequate, but ill-defined. According to (1.3) the phase speed is

$$c = \frac{\omega}{\xi},$$

but for the reflected parasite this formula gives a speed small and positive if ξ is considered to be slightly less than π/h, or small and negative if ξ is slightly less than $-\pi/h$. The difficulty is that since the wave is only observable at discrete time intervals, it cannot be said whether a sine wave has moved left or right to get from one configuration to the next. But whatever phase speed one selects will fail to capture the basic fact, that the edge of the parasite moves left at speed $\frac{5}{3}$.

This parasite, arising from the $(\pi/h, 0)$ corner of the dispersion plot, is of "saw/smooth" form—sawtoothed in x and smooth in t. Figures 1a–c suggest that smooth/saw and saw/saw parasites, arising from near $(0, \pi/k)$ and $(\pi/h, \pi/k)$ respectively, are also possible (under LF or LF4, though not under CN). Figure 6 confirms this for the scheme LF. In the same mesh as before, sinusoidal forcing functions with $\omega k = 0, 0.1, \pi$ are now turned on at $t = 0$ in the *middle* of the domain:

(Fig. 6a) $u(0, nk) \equiv 1$,
(Fig. 6b) $u(0, nk) = \sin(.1n)$,
(Fig. 6c) $u(0, nk) = (-1)^n$.

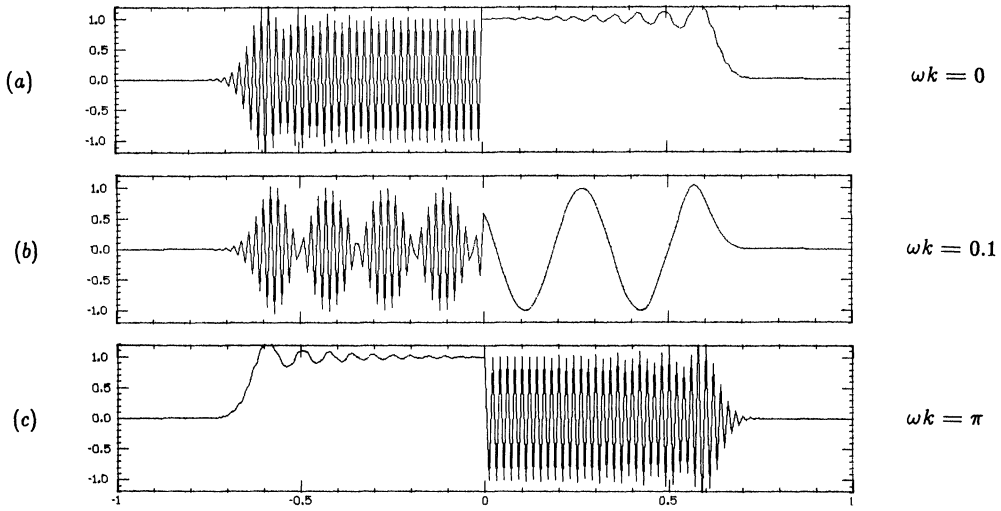

FIG. 6. *Generation of left- and rightgoing parasitic waves by a sinusoidal forcing function at the middle of an interval under* $u_x = -u_t$ *modeled by* LF *with* $\lambda = .5$. (*a*) $u(0, nk) \equiv 1$; (*b*) $u(0, nk) = \sin(.1n)$; (*c*) $u(0, nk) = (-1)^n$. *Each plot shows* $t = .66$.

This is an artificial experiment, since it amounts to specifying data on the outflow boundary of the interval $[-1, 0]$, but it highlights the completely predictable behavior of parasites. In Fig. 6a and 6b one sees saw/smooth and smooth/smooth waves on the left and right, respectively, just as in Fig. 5. In Fig. 6c the waves have become smooth/saw and saw/saw, although to display the sawtooth behavior in t it would be necessary to show an additional plot for $t = .66 + k$. All of these waves travel at group speeds approximately ± 1. The remarkable x symmetry in each plot is due to the ξ symmetry about $\xi = \pi/2h$ of Fig. 1c, and the t-symmetry relating Fig. 6a and 6c is due to the corresponding ω-symmetry. These details are unimportant, for they would change with the difference scheme. What is important is that smooth behavior in either x or t is no guarantee of smooth behavior in the other variable; that even extremely unphysical waves obey a group speed; and that this speed can easily have the wrong sign.

All of the dispersion plots of Fig. 1 leave large gaps of ω values for which there is no corresponding ξ. A difference scheme is incapable of propagating a wave of a frequency lying in such a "stop band" [16]. In a problem containing an interface, it may happen that a wave incident from one side has a frequency not sustainable on the other side, and in this event only an evanescent signal will be transmitted (cf. [3, Ch. 5], [5, Figs. 3–5], [16]). Such an interface might mark a coefficient change (as in Fig. 5), a change of difference scheme, or a refinement or coarsening of the mesh. To compute the cutoff frequency for transmission, one need only compute the value of ω at which C becomes 0 for the scheme at the far side. Of course, frequencies just below this cutoff, though they do get through the interface, will travel much too slowly.

In a problem solved with adaptive or fixed mesh refinement [5], [8], artificial interfaces appear at irregular places. As in Fig. 5, these interfaces may generate parasitic waves, which when the mesh refinement involves t as well as x can be sawtoothed in either variable [17]. This problem is usually overcome by the use of dissipative difference formulas [5]. But the possibility remains, in more than one space dimension especially, that a careless refinement strategy might cause substantial degradation of the qualitative nature of a wave solution due to errors in simulating

the primary (nonparasitic) wave. Suppose for example that part of a wave packet passes through a region of mesh refinement, and an adjacent part does not. If the two halves rejoin in the coarser mesh on the far side of the refined region, and if the meshes are not fine enough, then the first portion of the packet may have pulled substantially ahead of the second. This would be an effect of group speed. In a less severe case, the two halves may not separate significantly but may move apart in phase enough to cause interference when they rejoin. This would be an effect of phase speed. The latter problem is brought up at the end of the paper on mesh refinement by Browning, Kreiss and Oliger [5]. They do, not, however make the distinction between phase and group speed, even though an earlier derivation in that paper amounts to a calculation of the group speed, which is not the speed relevant to their interference discussion.

4. Group velocity in two dimensions. The extension of group speed to more than one dimension is surprisingly easy. In n dimensions, x and ξ become n-vectors $\mathbf{x}$ and $\boldsymbol{\xi}$, the dispersion relation takes the form

$$\omega = \omega(\boldsymbol{\xi}),$$

and C becomes a vector group velocity $\mathbf{C}$ given by the vector analogue of (1.5),

$$\mathbf{C} = \nabla_{\xi}\omega. \tag{4.1}$$

(∇_{ξ} denotes the gradient with respect to $\boldsymbol{\xi}$.) This formula is readily established by a stationary phase argument as in § 1 [12, § 4.4], [19, § 7.9]. Most nontrivial physical applications, of course, require more than one dimension. Moreover, problems in several dimensions will usually be modeled on a regrettably coarse mesh, so group velocity errors will be hard to avoid. (One important application area, in which group velocity problems are indeed conspicuous, is geophysical modeling of waves in the earth—see [2], [9].) Because of the anisotropy of the finite difference grid itself, (4.1) will imply that coarsely represented waves in multidimensional difference models travel not only at the wrong speed, but also in the wrong direction. In this respect a finite difference grid is analogous to a solid crystal, which also has preferred directions, and the effects we will discuss have well understood analogues in the crystal optics and acoustics literature [1], [3], [11].

For simplicity let us confine ourselves to two dimensions. Consider the second-order wave equation,

$$u_{tt} = u_{xx} + u_{yy}, \tag{4.2}$$

which we will model by the leap frog scheme LF^2:

$$U_{ij}^{n+1} - 2U_{ij}^{n} + U_{ij}^{n-1} = \lambda^2[U_{i+1,j}^{n} + U_{i-1,j}^{n} + U_{i,j+1}^{n} + U_{i,j-1}^{n} - 4U_{ij}^{n}] \tag{4.3}$$

on a rectilinear mesh with step size h in both x and y. The dispersion relation for (4.2) is the system of concentric circles

$$\omega^2 = \xi^2 + \eta^2 \tag{4.4}$$

(with $\boldsymbol{\xi} = (\xi, \eta)$), but for LF^2 this becomes after some trigonometic manipulations

$$\sin^2\frac{\omega k}{2} = \lambda^2\left[\sin^2\frac{\xi h}{2} + \sin^2\frac{\eta h}{2}\right]. \tag{4.5}$$

From a contour plot of this numerical dispersion relation, one can see the errors in group velocity that LF^2 will give rise to (cf. [1, Ch. 7], [11, Ch. 15]). Figure 7 shows

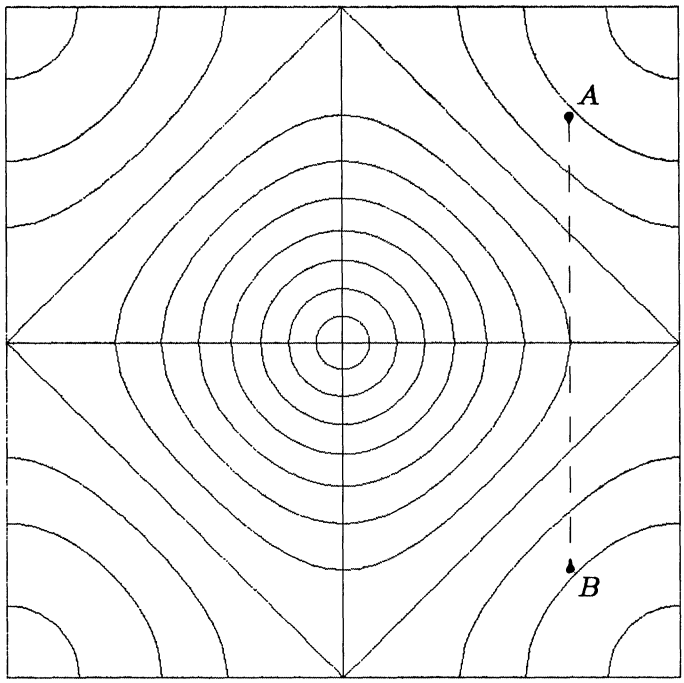

FIG. 7. *Dispersion plot for scheme* LF^2 *in the limit* $\lambda \to 0$. *The region shown is the domain* $[-\pi/h, \pi/h] \times [-\pi/h, \pi/h]$ *of the* $\xi = (\xi, \eta)$ *plane. The concentric curves plotted, beginning at the innermost near-circle, are lines of constant* ω *for* $\omega h = \pi/8, 2\pi/8, \cdots, 11\pi/8$. *The normal to such a curve at a point* ξ *is the group velocity direction for a packet of wave number* ξ. *For an explanation of the dashed line see the ray propagation example at the end of* § 4.

curves of constant ω in ξ-space for $\omega h = \pi/8, \cdots, 11\pi/8$. For simplicity λ has been taken here equal to 0, so that LF^2 is reduced to a semi-discrete or "method of lines" approximation. The full domain portrayed is $(\xi, \eta) \in [-\pi/h, \pi/h] \times [-\pi/h, \pi/h]$; any other wave number vector is an alias of a vector in this region. The figure shows that as ω increases, the curve of corresponding ξ vectors becomes less like a circle and more like a diamond. Now (4.1) implies that the group velocity for any wave number ξ points in the direction of the normal to the line of constant ω through ξ. By contrast the phase velocity, since it is normal to the wave front, lies along the ray from the origin through ξ, and so would the ideal group velocity for (4.2). Thus Fig. 7 indicates that poorly resolved wave packets will travel more along a diagonal under LF^2 than they ought to. The figure also shows an increasing separation between curves of constant ω as ω increases. By (4.1) this indicates that poorly resolved packets will travel too slowly, as in the one-dimensional case, and evidently this effect will be more pronounced at 0° or 90° than at 45°.

Applying (4.1) to (4.5) recapitulates these phenomena algebraically (cf. [2]). Here it is definitely simplest to perform the differentiation implicitly and settle for mixed forms involving both ω and ξ, as discussed at the end of § 2. One obtains the group velocity components

$$C_x = \frac{\lambda \sin \xi h}{\sin \omega k}, \qquad C_y = \frac{\lambda \sin \eta h}{\sin \omega k}. \tag{4.6}$$

Therefore the group propagation angle (from the x-axis) and speed for the wave

number vector (ξ, η) are

$$\Theta = \tan^{-1}\left(\frac{\sin \eta h}{\sin \xi h}\right), \tag{4.7a}$$

$$|\mathbf{C}| = \frac{\lambda\sqrt{\sin^2 \xi h + \sin^2 \eta h}}{\sin \omega k}. \tag{4.7b}$$

(Here $|\mathbf{C}|$ denotes $\sqrt{C_x^2 + C_y^2}$.) For infinitesimal ξh (4.7) reduces to the isotropic and nondispersive formulas

$$\Theta = \tan^{-1}\frac{\eta}{\xi}, \qquad |\mathbf{C}| = 1,$$

but for finite ξh it confirms that there is anisotropy and dispersion. Let θ denote the angle from the x-axis of the normal to a given plane wave. Then to second order

$$|\mathbf{C}| \approx 1 - \frac{(|\boldsymbol{\xi}|h)^2}{8}\left[\frac{3+\cos 4\theta}{4} - \lambda^2\right], \tag{4.8a}$$

$$\Theta \approx \theta + \frac{(|\boldsymbol{\xi}|h)^2}{24}\sin 4\theta. \tag{4.8b}$$

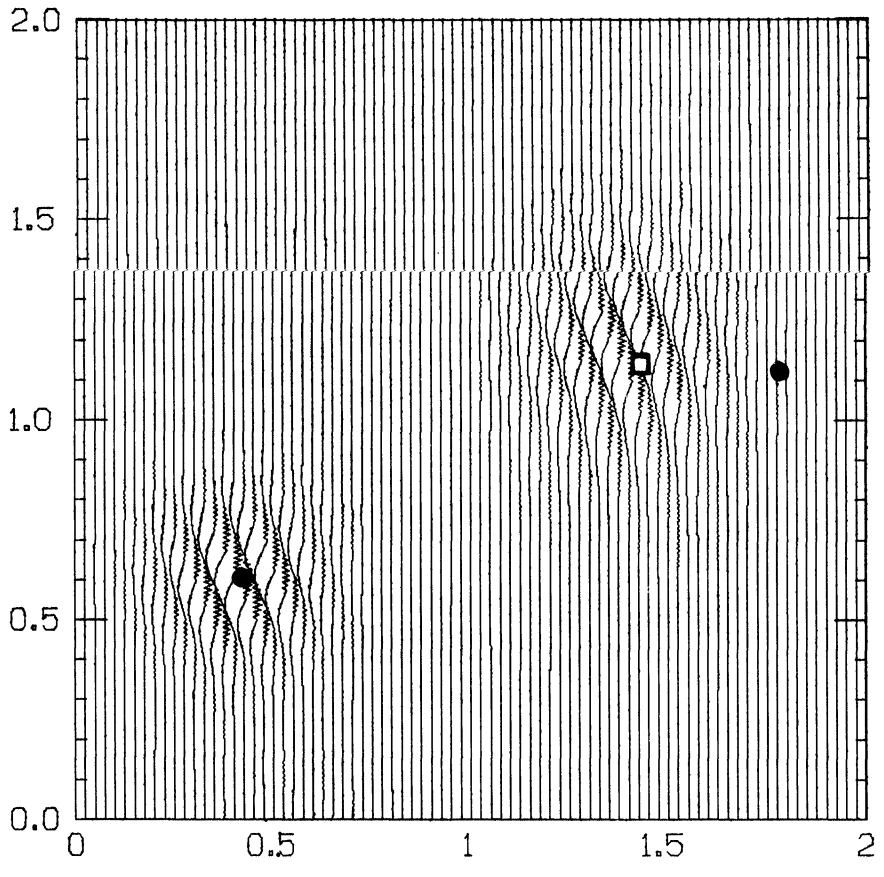

FIG. 8. *Propagation of a wave packet with* $|\boldsymbol{\xi}|h = 1.6$, $\theta = 22.5°$ *under* $u_{tt} = u_{xx} + u_{yy}$ *modeled by* LF^2 *with* $\lambda = .4$. *The packet is shown at both* $t = 0$ (*lower left*) *and* $t = 1.4$ (*upper right*). *Dots mark the ideal starting and ending positions, and the square the predicted position under* LF^2.

Equation (4.8a) shows again that waves will travel more slowly than the correct speed 1, lagging twice as much (for small λ) at $\theta \equiv 0°$ (mod 90°) as at $\theta \equiv 45°$ (mod 90°). Equation (4.8b) confirms that waves with $\theta \equiv 0°$ (mod 45°) will propagate perpendicularly to the wave front (a fact obvious from the symmetries of the grid), but that all other waves will propagate obliquely, preferring diagonals to horizontals and verticals. The details would change if the x and y mesh spacings were not equal.

Figure 8 confirms these predictions. Here a Gaussian wave packet

$$u(\mathbf{x}, 0) = \sin(\mathbf{x} \cdot \boldsymbol{\xi})\, e^{-30|\mathbf{x}|^2}$$

with $\theta = 22.5°$ and $|\boldsymbol{\xi}|h = 1.6$ has been set up at $t = 0$. The experiment takes $h = .01$, $\lambda = .4$, scheme $= \mathrm{LF}^2$. Superimposed on the same plot is the packet at the later time $t = 1.4$. Ideally it should have traveled a distance 1.4 at an angle 22.5°. In fact, it has closely matched the predictions of (4.7): $\Theta = 30.0°$, $|\mathbf{C}| = .81$.

A second illustration of anisotropy under LF^2 appears in Fig. 9, the two-dimensional analogue of Fig. 3. In the same grid as for Fig. 8, an initial quarter-circular

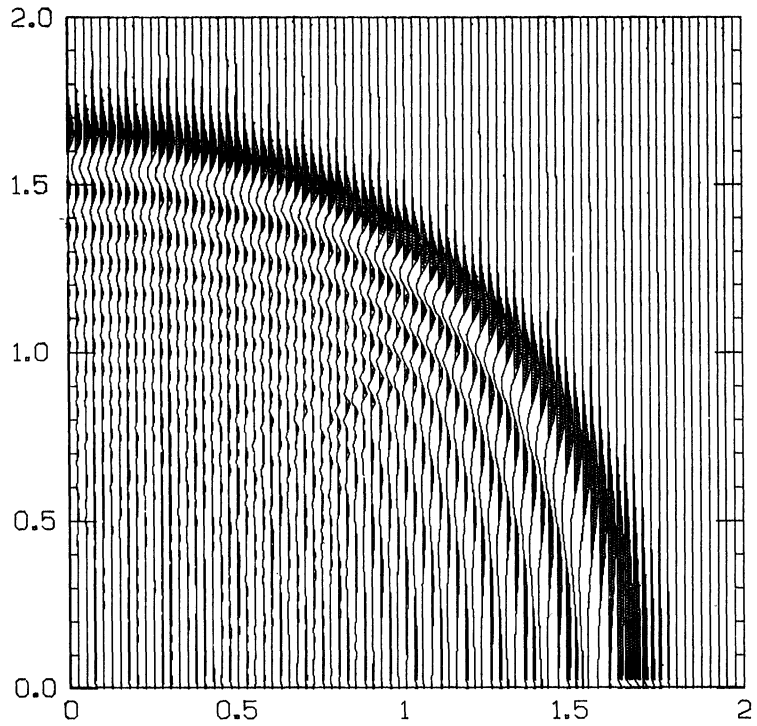

FIG. 9. *Propagation of an initial thin quarter-circular pulse to* $t = 1.4$ *under* $u_{tt} = u_{xx} + u_{yy}$ *modeled by* LF^2 *with* $\lambda = .4$ *The dispersion is twice as great at* 0° *and* 90° *as at* 45°.

pulse has been made to expand. The two levels of initial data were

$$u(\mathbf{x}, 0) = e^{-3600(|\mathbf{x}|-.3)^2}, \qquad u(\mathbf{x}, k) = e^{-3600(|\mathbf{x}|-(.3+k))^2}.$$

The figure shows the distribution at $t = 1.4$. The outer edge, containing low-frequency energy, has traveled at speed close to 1 and remains a circle. Within this shell, however, increasingly noncircular rings of higher wave number energy are visible. One can see that group speeds are greater at 45° than at 0° or 90° by the fact that a given separation

between rings (hence wave number $|\xi|$) appears farther from the origin at 45° than in other directions.

For comparison, Fig. 10 shows the same experiment conducted with a difference scheme designed to be more nearly isotropic. Let LF_2 denote the LF^2 scheme applied

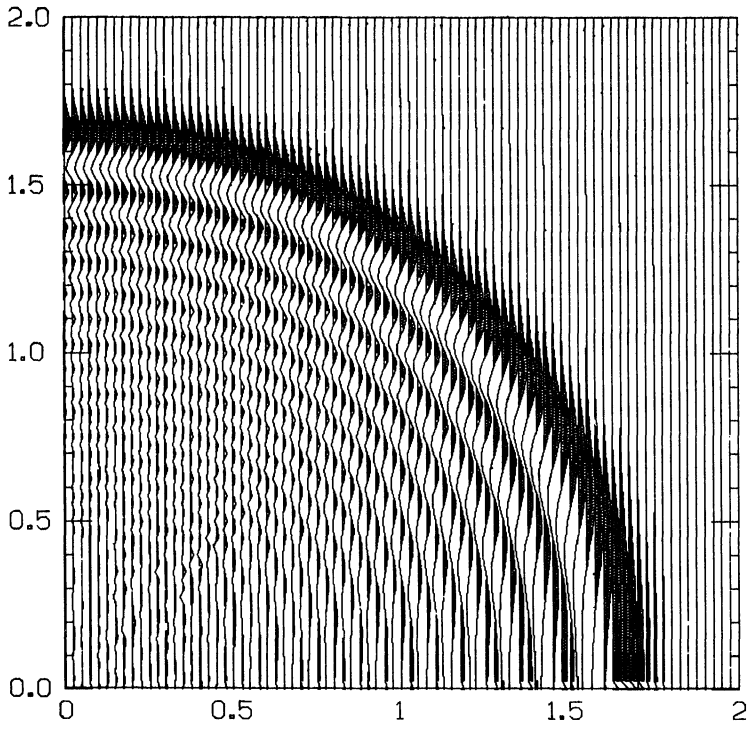

FIG. 10. *Same as Fig. 9 but with* LF^2 *replaced by a more nearly isotropic scheme. See text.*

on the same grid with a stencil inclined at 45°—hence with mesh size $\sqrt{2}h$. Taking a linear combination of LF^2 and LF_2 will tend to smear out the anisotropy of LF^2, and it is straightforward to show that the particular combination

$$\frac{2}{3}LF^2+\frac{1}{3}LF_2$$

is isotropic to order $(|\xi|h)^4$. Figure 10 shows the difference this makes in the expanding shell problem. The new scheme disperses waves at all angles as much (to fourth order) as LF^2 does at its worst angles, $\theta \equiv 0°$ (mod 90°); thus it is entirely worse than LF^2 from the point of view of truncation error. Yet it is easy to imagine that in some applications Fig. 10 would be a more satisfactory outcome than Fig. 9. The importance of isotropic difference formulas is considered in a paper of Watts and Silliman [18] for the problem of modeling flow in petroleum reservoirs.

In realistic problems, coefficients will usually vary in space. If the wavelengths of concern are small on the scale of the spatial inhomogeneity, then well-known ray tracing formulas will make it still possible to predict the errors introduced by finite differencing. Let the differential equation or difference approximation now have the dispersion relation

$$\omega = \omega(\mathbf{x}, \xi).$$

Then the ray tracing formulas for propagation of a wave packet are [12, § 4.5]

$$\frac{d\mathbf{x}}{dt} = \nabla_{\xi}\omega, \tag{4.9a}$$

$$\frac{d\boldsymbol{\xi}}{dt} = -\nabla_{x}\omega, \tag{4.9b}$$

$$\omega(t) = \text{const.} \tag{4.9c}$$

The significant change here is that a refraction formula (4.9b) has been added to the group velocity formula (4.9a). These equations reduce the ray tracing problem, for either the partial differential equation or the difference approximation, to the job of integrating an ordinary differential equation in $\mathbf{x}$ and $\boldsymbol{\xi}$.

As an example here is a problem in a stratified medium in two dimensions. Suppose that a wave packet at the origin, initially oriented at an angle $\theta(t=0)$ to the x axis, is made to propagate in the direction of increasing x under the equation

$$u_{tt} = a^2(y)(u_{xx} + u_{yy}). \tag{4.10}$$

Let $\boldsymbol{\xi} = (\xi, \eta)$ again. Because the problem is stratified, (4.9) can be simplified by observing that as the packet propagates, $\xi(t)$ as well as $\omega(t)$ will remain constant. Given $y(t)$, $\eta(t)$ can therefore be determined without integrating (4.9b) from the dispersion relation

$$\omega^2 = a^2(y)(\xi^2 + \eta^2)$$

for (4.10) itself or (in extension of (4.5))

$$\sin^2\frac{\omega k}{2} = a^2(y)\lambda^2\left[\sin^2\frac{\xi h}{2} + \sin^2\frac{\eta h}{2}\right] \tag{4.11}$$

for LF^2. This amounts to an application of Snell's law. The quantities $\dot{x}(t)$ and $\dot{y}(t)$ are then determined by (4.9a). Thus in the stratified case, (4.9a, b) reduce to an ODE for $\mathbf{x}$ alone.

In particular, take $\theta(0) = 45°$ and

$$a(y) = 1 + y^2.$$

For the differential equation, straightforward manipulations based on Snell's law give the ray equations

$$\dot{x}(t) = \frac{1}{\sqrt{2}}(1 + y^2(t))^2, \tag{4.12a}$$

$$\dot{y}(t) = \frac{(1 + y^2(t))^2}{\sqrt{(1 - 2y^2 - y^4)/2}}. \tag{4.12b}$$

For the approximation LF^2, one gets

$$\dot{x}(t) = (1 + y^2(t))\frac{\lambda \sin \xi h}{\sin \omega k}, \tag{4.13a}$$

$$\dot{y}(t) = (1 + y^2(t))\frac{\lambda \sin \eta(t) h}{\sin \omega k}, \tag{4.13b}$$

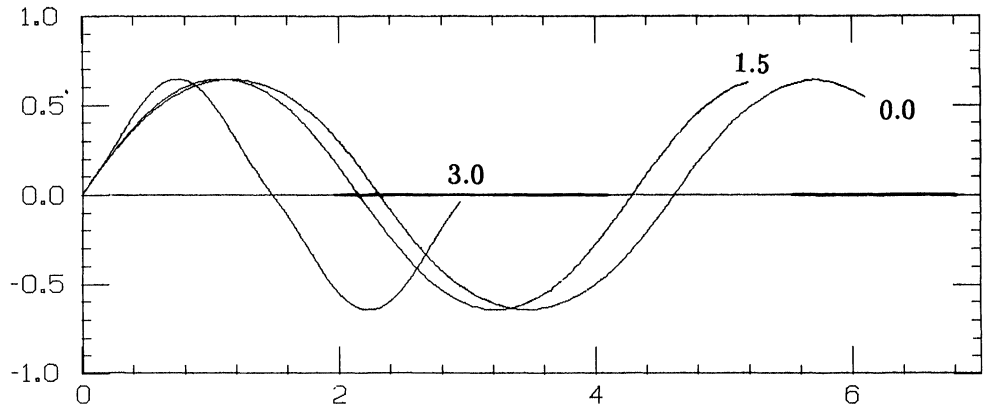

FIG. 11. *Predicted rays for the wave packet of* § 4 *when modeled by* LF^2 *with* $\lambda = .25$ *for* $|\xi|h = 0$ *(exact solution),* 1.5, *and* 3.0. *Each ray goes from* $t = 0$ *to* $t = 6$. *As the mesh becomes coarser the group speed reduces and the path approaches a zig-zag.*

with $\eta = \eta(\omega, \xi, y)$ determined by (4.11). Figure 11 shows numerically calculated ray paths predicted by (4.13) with $\lambda = .25$ for wave numbers $|\xi|h = 0, 1.5, 3$. The ideal solution, corresponding to $|\xi|h = 0$, is an oscillatory path that varies smoothly between $(\sqrt{2}-1)^{1/2} \approx \pm .6436$. As $|\xi|h$ increases, indicating a more and more coarsely resolved wave packet, the ray approximates a zig-zag between the same limits instead. This is another reflection of the favored role of diagonals under LF^2.

The dashed line in Fig. 7 gives a more intuitive explanation of where the zig-zag behavior comes from (although Fig. 7 represents $\lambda = 0$, not $\lambda = .25$). The initial packet with $|\xi|h = 3.0$ has the wave number vector marked A. As the packet traverses the ray up, down and up again, ξ crosses the ξ-axis, hits point B, then returns to the ξ-axis. The path in ξ-space is a straight line segment because $\xi(t)$ remains constant. The frequency $\omega(t)$ is also constant, but as $a^2(y(t))$ changes, the frequency that each contour line in Fig. 7 corresponds to changes, so the line AB appears to cross frequency contours. One can see that the group propagation angle will begin at $\Theta = 45°$, then actually increase slightly above this figure before falling below it. Sure enough, this effect is visible in Fig. 11. Computational experiments with a wave packet like that of Fig. 8 also confirm all of these predictions.

5. Group velocity and stability. For a finite difference model to be useful it must be stable as well as accurate, which means that small errors (such as rounding errors) must have no possibility of growing uncontrollably and thereby obliterating the correct solution. For pure initial value problems, in which a differential equation is solved in an unbounded spatial domain, the question of stability is well understood theoretically [13], [15]. For initial boundary value problems, however, the situation is much more complicated. The purpose of this section is to point out that the stability or instability of a difference model of an initial boundary value problem has a natural connection with what group velocities the model can support.

The best available stability theory for such models appeared a decade ago in an important but difficult paper of Gustafsson, Kreiss, and Sundström—henceforth GKS [10]. This theory is truly complicated, so our remarks will not attempt rigor or full generality, but will focus on the simplest (and most important) case that it resolves. Several of the cases that remain are associated with group velocities $C = 0$, and are not well treated by the GKS theory, which because of an unnaturally strict stability

definition rules at least some such problems unstable that are really stable. An example of this kind will be given at the end.

Consider the first-order hyperbolic system

$$u_t = Au_x + F(x, t) \tag{5.1a}$$

on the quarter-plane $x, t \geqq 0$, where u and F are N-vectors and A is a constant $N \times N$ matrix. Assume that A has the form

$$A = \begin{bmatrix} -A_{\mathrm{I}} & 0 \\ 0 & A_{\mathrm{II}} \end{bmatrix}$$

where A_{I} is $N_{\mathrm{I}} \times N_{\mathrm{I}}$, A_{II} is $N_{\mathrm{II}} \times N_{\mathrm{II}}$, and both are Hermitian and positive definite. Appropriate initial and boundary conditions for this system are

$$u(x, 0) = f(x), \qquad u^{\mathrm{I}}(0, t) = Su^{\mathrm{II}}(0, t) + g(t), \tag{5.1b}$$

where u^{I} and u^{II} make up a partition of u corresponding to the partition of A, and S is a constant $N_{\mathrm{I}} \times N_{\mathrm{II}}$ matrix. Let (5.1) be modeled on a uniform h-k grid by a fixed "interior" formula at all points $x_\nu \geqq rh$ together with r "boundary" formulas for the points $x_0, \cdots, x_{r-1}$. Assume that the interior formula is Cauchy stable—that is, it would be stable if applied for all x in a pure initial value problem. Denote the combined difference operator in the homogeneous case by Φ, so that

$$U^{n+1} = \Phi U^n$$

when $F \equiv g \equiv 0$. For simplicity assume that Φ is constant independent of the mesh size h, and that $k = \lambda h$ for all h with λ constant.

The basis of most stability theories for difference models is normal mode analysis, the study of eigensolutions of the difference operator: that is, of spatial distributions ϕ_ν with the property that $U_\nu^n = z^n \phi_\nu$ is a solution of the homogeneous difference model, for some complex constant z. The idea is that if an eigensolution with $|z| > 1$ exists that might be excited by random errors, then the model is unstable. The mathematical complexities come in pinning down what it means to be excitable by such errors, and in determining how close the criterion $|z| \leqq 1$ is to being a sufficient as well as necessary condition for stability.

Let us begin with the easiest case, which requires neither group velocity nor the GKS theory. Suppose there exists an eigensolution $\phi = (\phi_0, \phi_1, \cdots) \in l_2$ of the difference model Φ, i.e.,

$$(\Phi\phi)_\nu = z\phi_\nu \quad \forall \nu \geqq 0, \tag{5.2}$$

with $|z| > 1$. This equation must hold not only in the interior, but also at the boundary points $x_0, \cdots, x_{r-1}$. Since $\phi \in l_2$ the rounding error at a given step might in principle be a small multiple of ϕ; in general, a random error distribution must be expected to include a small component of ϕ. This component will immediately begin to grow like $|z|^n$, and for small enough h, k, the growth is more rapid than $e^{\alpha t}$ for any fixed α. This is an unambiguous kind of instability, and in practice if such an eigensolution exists in a computation, it will almost always overwhelm the correct solution rapidly. We have shown:

GODUNOV-RYABENKII (G-R) CONDITION [10], [13]: *A necessary condition for stability of an initial boundary value problem model is that there exist no eigensolution* $\phi \in l_2$ *with* $|z| > 1$.

Now consider the possibility $|z| = 1$. Suppose that for some complex number κ with $|\kappa| = 1$, the difference model admits an eigensolution of the form

$$\phi_\nu = \kappa^\nu \psi$$

for some N-vector ψ. In this case $\phi \notin l_2$, so it is no longer clear whether random errors must contain a component of ϕ, and since $|z| = 1$, it does not appear that such errors will grow anyway. Let us sidestep these issues by considering the function

$$U_\nu^0 = \begin{cases} \phi_\nu & \text{for } x_\nu \leqq M, \\ 0 & \text{for } x_\nu > M \end{cases}$$

for some constant M. U^0 is not an eigensolution of Φ, for it will change form at each time step. Near $x = 0$, it will behave like ϕ, and for $x \gg M$ it will remain 0. What happens near $x = M$, however, depends on the group velocity. Write $z = e^{i\omega k}$ and $\kappa = e^{i\xi h}$. Since ϕ is an eigensolution, ω and ξ satisfy the dispersion relation for the interior scheme, and under normal circumstances the corresponding group velocity $C = d\omega/d\xi$ exists and is real. Then as $t \to \infty$, the wave front at $x = M$ will retreat into the boundary if $C < 0$ and advance steadily into $x \geqq 0$ if $C > 0$. In the latter case, we have a polynomially growing instability. The initial l_2 norm is then $\|U^0\|_2 = \sqrt{M}\|\psi\|_2$, but evidently it will grow as $t \to \infty$ according to $\|U^n\|_2 \approx \sqrt{M + Ct}\|\psi\|_2$. Since M may be arbitrarily small (provided h is decreased correspondingly to maintain $h \ll M$), this growth is an unbounded function of the initial distribution.

More generally, suppose that the difference model has an eigensolution

$$\phi_\nu = \sum_{i=1}^{j} \kappa_i^\nu \psi_i, \tag{5.3}$$

with $|\kappa_i| = 1$ for each i and $|z| = 1$. Assume that for each i, C_i exists and satisfies $C_i > 0$. Then again we have a polynomially growing instability. One may express this as follows:

G-R Condition Extension. *A necessary condition for stability of an initial boundary value problem model is that there exist no eigensolution of the form* (5.3) *consisting entirely of outgoing waves – that is, of waves with* $C_i > 0$.

In practice an instability of this kind will often but not always cause trouble in a realistic computation, since its polynomial growth is relatively slow. When more than one boundary is present, however, repeated reflections back and forth may sometimes convert the polynomial growth to exponential [10].

Let us now look at an example, then turn to the GKS theory proper and to some of the complexities we have glossed over, and finally concentrate on some difficulties associated with $C = 0$.

Suppose we set out to solve the scalar problem $u_t = u_x$ on $x, t \geqq 0$ by applying LF or CN for $x_\nu \geqq h$. With either of these schemes we need a boundary formula for the point $x_0 = 0$. Almost any formula will satisfy the G-R condition, but many will violate the extension. In particular, consider the possibilties

BC1: $U_0^{n+1} = U_1^{n+1}$,
BC2: $U_0^{n+1} = U_1^n$,
BC3: $U_0^{n+1} = U_2^{n-1} + (\lambda - 1)(U_2^n - U_0^n)$.

From Fig. 1 it is apparent that CN admits a rightgoing parasite with $(\xi h, \omega k) = (\pi, 0)$, and LF admits this and also a rightgoing parasite with $(\xi h, \omega k) = (0, \pi)$. If either of these waves satisfies the boundary condition, the model is unstable. Now the $(\pi, 0)$

wave is sawtoothed in x and constant in t, so it does not satisfy BC1 or BC2. But it does satisfy BC3, from which we conclude

Unstable: LF or CN with BC3.

Similarly, the $(0, \pi)$ wave satisfies both BC1 and BC3, which implies

Unstable: LF with BC1 or (again) BC3.

Of course we have not examined all potential outgoing eigensolutions, nor shown that the absence of them implies stability, but it turns out that the cases not excluded above are indeed stable: LF or CN with BC2, and CN with BC1 [10, § 6]. Note especially that the wave with $(\xi h, \omega k) = (\pi, \pi)$ is an eigensolution of LF with BC2, but it has $C = -1 < 0$, so this is not an indication of instability. The same goes for the constant wave $(\xi h, \omega k) = (0, 0)$ with any scheme and any boundary condition.

How does all of this relate to the GKS theory? The theory is built around a rigorous treatment of eigensolutions ϕ with $|z| = 1$. It shows first that every such ϕ can be resolved algebraically in terms of characteristic values κ_i of the interior difference formula, as in (5.3). But where we have asked whether $C_i > 0$ for the case $|z| = |\kappa_i| = 1$, GKS consider the algebraic question: when $|z| = 1$ is perturbed to the outside of the unit circle, does κ_i move to $|\kappa_i| < 1$ or to $|\kappa_i| > 1$? (The possibility $|\kappa_i| = 1$ is excluded by the Cauchy stability of the interior scheme.) It is easy to see that when $C_i = d\omega/d\xi_i$ exists and is real, with $z = e^{i\omega k}$ and $\kappa_i = e^{i\xi_i h}$, then $C_i > 0$ implies the former and $C_i < 0$ the latter. Thus the GKS condition is, roughly, a condition on group velocities. The difference is that there are many cases covered by the GKS approach that do not directly fit the group velocity formulation. First, (5.3) is generalized to allow the possibility of defective characteristic values κ_i. Second, the theory allows for the possibility $|\kappa_i| < 1$, $|z| = 1$, which it holds to be unstable. Third, it does not require $C = d\omega/d\xi$ to exist or be real, and when C exists but is zero it rules the model stable or unstable according to the behavior under perturbation. All together, the main theorem states:

GKS THEOREM. *An initial boundary value problem model is stable if and only if there exists no eigensolution with* $|z| \geqq 1$ *and* $|\kappa_i| \leqq 1$, *where in the case* $|z| = |\kappa_i| = 1$ *one admits only those* κ_i *which perturb to* $|\kappa_i| < 1$ *for* $|z| > 1$.

Eigensolutions of the latter kind are properly called *generalized eigensolutions.*

On the face of it, then, whereas the G-R condition and its extension are only partial results, the GKS theory completes the study of stability by establishing a necessary and sufficient condition. But it turns out that in order to achieve this, the theory adopts a very strict definition of stability [10, Def. 3.3], under which some eigensolutions with $C_i = 0$ are found to be unstable that in fact do not grow with t in the l_2 norm. Here is an example.

Let $u_x = u_t$ be solved by LF on the entire real line $x \in (-\infty, \infty)$. This is not a boundary value problem, but we can pretend it is one by writing it as the equivalent vector system

$$\begin{pmatrix} u \\ v \end{pmatrix}_t = \begin{pmatrix} 1 & 0 \\ 0 & -1 \end{pmatrix} \begin{pmatrix} u \\ v \end{pmatrix}_x, \qquad u(0) = v(0) \tag{5.4}$$

on $x, t \geqq 0$, and solving this with the LF formula for $x_\nu \geqq h$ together with boundary conditions that mimic LF at $x_0 = 0$,

$$U_0^{n+1} - U_0^{n-1} = \lambda (U_1^n - V_1^n), \qquad V_0^{n+1} - V_0^{n-1} = \lambda (U_1^n - V_1^n).$$

This trick of "folding" an initial value problem into an initial boundary value problem is a standard one for analyzing stability in problems with discontinuities or interfaces

[5], [8], [14]. Here we have the degenerate case of a completely transparent interface. Now LF is well known to be stable in the l_2 norm for $u_t = v_x$ on $(-\infty, \infty)$. Yet according to the GKS theory, our model for (5.4) is unstable! The numbers $\kappa_u = \pm i$, $\kappa_v = \mp i$, $z = \exp(\pm i \sin^{-1}\lambda)$ can be seen to define an eigensolution such that when z is perturbed to $|z| > 1$, the effect is $|\kappa_u| < 1$ and $|\kappa_v| < 1$. This is a case with $C_u = C_v = 0$.

The explanation for the apparent paradox is that the GKS stability definition essentially requires the norm

$$\|U\|^2 = k \sum_{n=0}^{\infty} |U_0^n|^2 + hk \sum_{\nu,n=0}^{\infty} |U_\nu^n|^2 \tag{5.5}$$

of the computed solution to be uniformly bounded in terms of the initial data. This norm is unusual in that it measures U not only in the field $x, t \geqq 0$, but also as an integral along the boundary $x = 0$. For any difference model that permits $C(\xi) = 0$ for some ξ, hence for almost any nondissipative method, the possibility exists that an initial distribution dominated by such ξ will accumulate in a sharp stationary spike at $x = 0$, and then it will be impossible to contain the growth of the left-hand sum in (5.5). Figure 12 shows an experiment contrived to make exactly this happen. The idea is that if one sets up initial data with a local wave number distribution satisfying

$$C(\xi(x)) = -\frac{x}{T}, \tag{5.6}$$

then energy from each point will have moved to the origin at time T. For LF $C(\xi)$ is given by (2.2a), and (5.6) becomes after some manipulations

$$\xi h = \sin^{-1}\sqrt{\frac{x^2 - T^2}{\lambda^2 x^2 - T^2}}.$$

An initial signal with this wave number distribution,

$$U(x, k) = U(x, 0) = 0.1 \sin\left[\int_0^x \xi(s)\, ds\right],$$

appears in Fig. 12a (with $T = .75$). (The integral was evaluated numerically.) Figures 12b–d show the configuration at times $t = .9T = .675$, $t = T = .75$, and $t = 1.1T = .825$. As intended, a spike of magnitude approaching

$$U(0, t) = \frac{0.1}{\sqrt{|1 - t/T|}}$$

evidently forms at $x = 0$, and since this function diverges in the norm (5.5) as $k \to 0$, the LF model for (5.4) is indeed unstable in the GKS norm, even though it is stable in l_2.

It is clear enough that this transparent interface problem is a degenerate one, since we can show it is l_2-stable by the more elementary theory of initial value problem models. But one can devise boundary formulas that permit eigensolutions with $C = 0$ which are not susceptible to such an argument. One example of this appears with the equation $u_t = u_x$ on $x, t \geqq 0$ modeled by LF with $\lambda = .5$ and the (bizarre) boundary condition $U_0^{n+1} = U_1^{n-2}$. The GKS theory calls this model unstable, but it is not clear what kind of growth there is really a danger of.

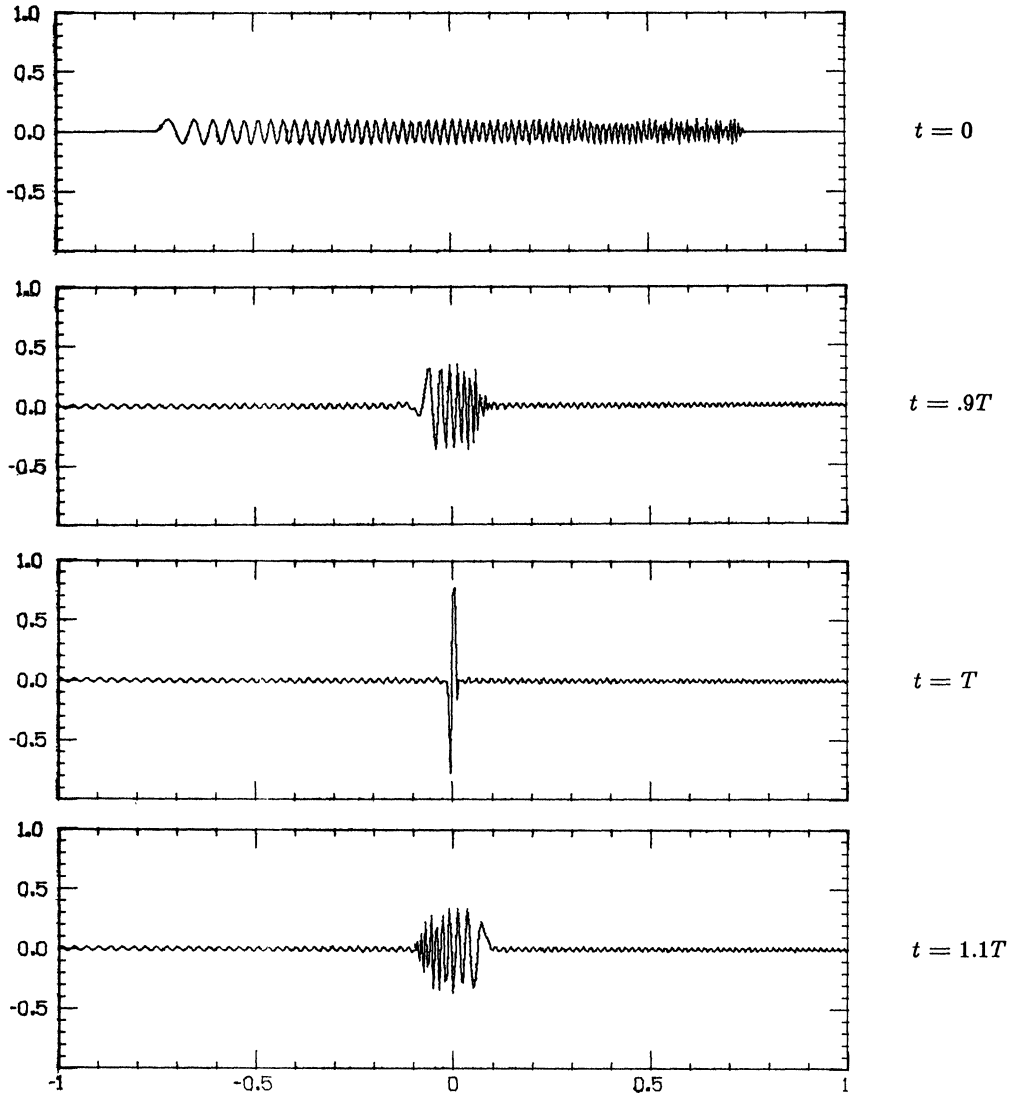

FIG. 12. *Formation of a spike at the origin under* LF *with* $h = .005$, $\lambda = .5$. *The initial distribution is chosen so as to make the spike appear at* $t = T = .75$. *According to the norm of Gustafsson, Kreiss, and Sundström, this possibility makes* LF *unstable for the Cauchy problem if* $x = 0$ *is thought of as an interface point.*

To summarize this section, we have found a connection between the instability of a discrete model of an initial boundary value problem and the possibility that a set of waves with $C > 0$ can radiate from the boundary without being stimulated by incoming waves with $C < 0$. Since group velocity governs the flow of energy, and instability is related to the uncontrolled creation of energy, it is not surprising that there should be such a connection. We have also found that borderline cases with $C = 0$ are not satisfactorily treated by existing theory. This is also not surprising, as these cases are the numerical analogues of initial boundary problems with characteristic boundaries, and the theory of such problems is well known to have complications of its own.

6. Summary. Why worry about group velocity in finite difference schemes? One answer is that by doing so, one can obtain a great deal of insight with a small amount

of effort. We have done little here besides write down dispersion relations and differentiate them, yet the result has been a quantitative understanding of differencing errors in wave propagation problems, of the appearance of parasitic waves, of the anisotropic behavior of multidimensional difference schemes, and of instability in initial boundary value problems. Many more matters related to group velocity could also be pursued, particularly with regard to amplitude and energy propagation; as usual, the difference model introduces systematic errors here, which become particularly interesting in problems involving reflection and transmission at real or artificial interfaces.

The major omission from the practical point of view has been our neglect of dissipative difference formulas. All finite difference models are dispersive, but many are dissipative as well. Dissipation makes wave packets not only travel at the wrong speed, but also decay with time. It also eliminates most parasitic waves by turning them into rapidly attenuating waves. Nevertheless, boundaries can still introduce instability. For many difference schemes dispersion dominates dissipation, and the effects of dissipation on group velocity can be added as higher-order corrections to the results obtained by ignoring it. However, an exact treatment is more complicated. One must now consider a complex dispersion relation, and replace the stationary phase argument with an argument of steepest descent [4], [6].

It is worth mentioning explicitly that the examples given here have involved larger errors than would be tolerated in realistic computations. In a finer grid, group speed errors might be 1%, not 25%; parasites generated at interfaces might be ten times weaker than in Fig. 5; dispersion as pronounced as in Fig. 3 and 8 would be out of the question. We have focused on pathologies to bring out the general principles. Indeed, our concern has been to identify phenomena rather than to compare the relative merits of particular discretization methods in practical applications. For comparisons of this kind see [2], [7], [17].

Here is a summary of the points that have been raised here. Once again: h = spatial grid size, ω = frequency, ξ = wave number.

§ 1: *Dispersion relations and group velocity*
- Difference models, even of nondispersive equations, are dispersive.
- Their dispersion relations are periodic, nonlinear, and in general multiple-valued.
- Wave crests travel at the phase speed $c = \omega/\xi$.
- Energy travels at the group speed $C = d\omega/d\xi$.

§ 2: *Pulses, wave packets, and wave fronts*
- c typically lags the correct speed like $(\xi h)^2$.
- C typically lags by 3 times as much.
- Wave packets and wave fronts travel at the group speed.
- Wave number dependent group speeds account for numerical dispersion.
- Lack of conspicuous dispersion does not assure correct propagation speed.
- Some analyses require $C = C(\xi)$, others $C = C(\omega)$.
- The simplest formulas for C mix both ξ and ω.

§ 3: *Parasites, interfaces, and mesh refinement*
- Sawtoothed parasites may be generated at interfaces, shocks, or other discontinuities.
- Parasites also obey a group speed, which often has the wrong sign.
- Group speed is the only meaningful speed for parasites.
- Smoothness in x or t does not imply smoothness in the other variable.

- $C(\omega) = 0$ defines a cutoff frequency for transmission through an interface.
- Insufficiently cautious mesh refinement can cause distinct problems related to both phase and group speed.

§ 4: *Group velocity in two dimensions*

- Difference methods in several space dimensions are anisotropic.
- Wave packets travel at the vector group velocity $\mathbf{C} = \nabla_{\xi}\omega$.
- Poorly resolved packets travel at the wrong speed *and* direction.
- Differencing errors in heterogeneous media can be predicted by standard ray tracing formulas.
- A numerical Snell's law holds for stratified problems.
- Group velocities can be inferred from a contour plot of the vector dispersion relation.

§ 5: *Group velocity and stability*

- Instability of an initial boundary value problem model is related to the possibility of radiating outgoing waves at the boundary ($C > 0$) that are not stimulated by incoming waves.
- A condition of Gustafsson, Kreiss, and Sundström is in part an algebraic formulation of this relationship.
- Different wave form and group speed combinations correspond to qualitatively different kinds of instabilities.
- When all group speeds are zero a GKS instability may be spurious.

Acknowledgments. This project has benefited tremendously from the generous advice of Gerald Hedstrom, who corrected several of my misconceptions and is patiently working on those that remain. I am also grateful for help of many kinds to Marsha Berger, Russel Caflisch, Raymond Chin, William Coughran, Jr., William Gropp, Randall LeVeque, and especially Joseph Oliger. Computations were performed at the Stanford Linear Accelerator Center of the U.S. Department of Energy.

REFERENCES

[1] B. AULD, *Acoustic Fields and Waves in Solids*, Wiley-Interscience, New York, 1973.
[2] A. BAMBERGER, G. CHAVENT AND P. LAILLY, *Etude de schémas numériques pour les équations de l'élastodynamique linéaire*, Res. Rep. 41, INRIA, France, 1980.
[3] L. BRILLOUIN, *Wave Propagation in Periodic Structures*, Dover, New York, 1953.
[4] ———, *Wave Propagation and Group Velocity*, Academic Press, New York, 1960.
[5] G. BROWNING, H.-O. KREISS AND J. OLIGER, *Mesh refinement*, Math. Comp., 27 (1973), pp. 29–39.
[6] R. CHIN AND G. HEDSTROM, *A dispersion analysis for difference schemes: Tables of generalized Airy functions*, Math. Comp., 32 (1978), pp. 1163–70.
[7] R. CHIN, G. HEDSTROM AND K. KARLSSON, *A simplified Galerkin method for hyperbolic equations*, Math. Comp., 33 (1979), pp. 647–658.
[8] M. CIMENT, *Stable difference schemes with uneven mesh spacings*, Math. Comp., 25 (1971), pp. 219–227.
[9] J. CLAERBOUT, *Fundamentals of Geophysical Data Processing*, McGraw-Hill, New York, 1976.
[10] B. GUSTAFSSON, H.-O. KREISS AND A. SUNDSTRÖM, *Stability theory of difference approximations for initial boundary value problems II*, Math. Comp., 26 (1972), pp. 649–686.
[11] F. JENKINS AND H. WHITE, *Fundamentals of Physical Optics*, McGraw-Hill, New York, 1937.
[12] J. LIGHTHILL, *Waves in Fluids*, Cambridge University Press, Cambridge, 1978.
[13] R. RICHTMYER AND K. MORTON, *Difference Methods for Initial-value Problems*, Wiley-Interscience, New York, 1967.
[14] A. SUNDSTRÖM, *Efficient numerical methods for solving wave propagation equations for non-homogeneous media*, Swedish Defense Inst. Rep. FOA 4 C 4576-A2, 1974.
[15] V. THOMÉE, *Stability theory for partial difference operators*, this Review, 11 (1969), pp. 152–195.

[16] R. VICHNEVETSKY, *Propagation properties of semi-discretizations of hyperbolic equations*, Math. Comput. Simulation, 22 (1980), pp. 98–102.

[17] R. VICHNEVETSKY AND B. PEIFFER, *Error waves in finite element and finite difference methods for hyperbolic equations*, in Advances in Computer Methods for Partial Differential Equations, R. Vichnevetsky, ed., Assoc. Int. Calcul Analogique, Ghent, Belgium, 1975, pp. 53–58.

[18] J. WATTS AND W. SILLIMAN, *Numerical dispersion and the origins of the grid-orientation effect: A summary*, Proc. 73rd Annual Meeting, AIChE, Chicago, 1980.

[19] G. WHITHAM, *Linear and Nonlinear Waves*, Wiley-Interscience, New York, 1974.